

SCIENTIFIC REPORTS

OPEN

Dimethylmercury Formation Mediated by Inorganic and Organic Reduced Sulfur Surfaces

Received: 08 March 2016

Accepted: 27 May 2016

Published: 15 June 2016

Sofi Jonsson^{1,2}, Nashaat M. Mazrui¹ & Robert P. Mason¹

Underlying formation pathways of dimethylmercury ((CH₃)₂Hg) in the ocean are unknown. Early work proposed reactions of inorganic Hg (Hg^{II}) with methyl cobalamin or of dissolved monomethylmercury (CH₃Hg) with hydrogen sulfide as possible bacterial mediated or abiotic pathways. A significant fraction (up to 90%) of CH₃Hg in natural waters is however adsorbed to reduced sulfur groups on mineral or organic surfaces. We show that binding of CH₃Hg to such reactive sites facilitates the formation of (CH₃)₂Hg by degradation of the adsorbed CH₃Hg. We demonstrate that the reaction can be mediated by different sulfide minerals, as well as by dithiols suggesting that e.g. reduced sulfur groups on mineral particles or on protein surfaces could mediate the reaction. The observed fraction of CH₃Hg methylated on sulfide mineral surfaces exceeded previously observed methylation rates of CH₃Hg to (CH₃)₂Hg in seawaters and we suggest the pathway demonstrated here could account for much of the (CH₃)₂Hg found in the ocean.

Dimethylmercury is a volatile and highly toxic form of mercury (Hg)¹. It appears to be ubiquitous in marine waters and has been found in deep hypoxic oceanic water, coastal sediments and upwelling waters and in the mixed layer of the Arctic ocean^{2–6}. Reported concentrations of (CH₃)₂Hg in marine waters range from 0.01–0.4 pM and (CH₃)₂Hg has been found to constitute a significant fraction (up to 80%) of the methylated Hg pool (CH₃Hg + (CH₃)₂Hg)^{1,6}. The role of (CH₃)₂Hg in the biogeochemical cycle of mercury, and its bioaccumulative potential, is not well known^{6–8}. However, for oceanic systems, and for the marine boundary layer, it has been suggested that degradation of (CH₃)₂Hg is an important source of CH₃Hg^{5,9,10}.

Monomethylmercury (CH₃Hg^{II}X⁻¹ where X is Cl⁻¹, OH⁻¹, R-S⁻¹ etc., here referred to as CH₃Hg) is known to bioaccumulate in aquatic food webs to concentrations of concern for human and wildlife health¹. Understanding the methylation processes of Hg has thus been a key objective for comprehending the factors influencing its biogeochemical cycle. Formation of CH₃Hg and (CH₃)₂Hg by aquatic organisms was first observed by Jensen and Jernelov in 1969¹¹. A large number of bacterial strains have since been tested for their ability to methylate Hg, primarily focusing on CH₃Hg formation. A corrinoid type protein and a 2[4Fe-4S] ferredoxin protein encoded by the HgcA and HgcB gene, respectively, was recently identified as essential for CH₃Hg production by anaerobic bacteria¹². The number of bacterial strains tested for their ability to methylate Hg to (CH₃)₂Hg is however limited and the main process remains to be identified^{13,14}.

In culture studies with *Desulfovibrio desulfuricans*, Baldi and his coworkers, observed production of (CH₃)₂Hg in parallel with a white precipitate following high additions of CH₃Hg(aq)¹⁴. This white precipitate was identified as dimethylmercury sulfide, (CH₃Hg)₂S(s). Previous work had shown (CH₃Hg)₂S(s) formation from the reaction between CH₃Hg(aq) and H₂S, and with time, its degradation to metacinnabar (β-HgS(s)) and (CH₃)₂Hg¹⁵. Baldi and his coworkers thus suggested the production of (CH₃)₂Hg by bacteria as an effect of sulfidogenic growth. Currently, the known pathways of (CH₃)₂Hg formation relevant to field conditions include reaction of CH₃Hg(aq) with H₂S¹⁵ or selenoaminoacids¹⁶ and methylation with methylcobalamin¹⁷. Computational calculations suggest a possible formation pathway from CH₃Hg complexed to L-cysteine, however experimental data is lacking¹⁸. With a up to 90% of the CH₃Hg in marine waters naturally occurring adsorbed to reduced sulfur groups on minerals

¹Department of Marine Sciences, University of Connecticut, 1080 Shennecossett Road, Groton, CT06340, USA.

²Centre for Environment and Sustainability, University of Gothenburg, Box 170, SE-405 30, Gothenburg, Sweden. Correspondence and requests for materials should be addressed to S.J. (email: sofijon84@gmail.com)

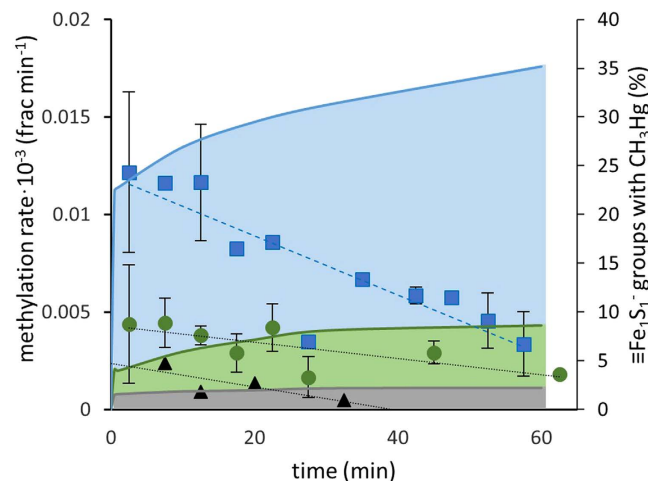


Figure 1. Methylation of CH_3Hg at different $\text{CH}_3\text{Hg}:\text{FeS}_m(s)$ ratios. Methylation rate of CH_3Hg (fraction min^{-1} , scatter plot, left hand axis) and percent of $\equiv\text{Fe}_1\text{S}_1^-$ groups on the $\text{FeS}_m(s)$ surface with CH_3Hg adsorbed (background area graph, right hand axis) at $\text{CH}_3\text{Hg}:\text{FeS}_m(s)$ ratios ($\text{nmol } \mu\text{mol}^{-1}$) of 3.9 (blue squares, upper blue area), 1.0 (green circles, middle green area) and 0.25 (black triangles, lower gray area). Methylation rates at the three $\text{CH}_3\text{Hg}:\text{FeS}_m(s)$ ratios tested were significantly different ($p < 0.05$, Analysis of Covariance).

or bound to thiols on organic matter, surface mediated processes are of interest. We therefore hypothesized that $(\text{CH}_3)_2\text{Hg}$ could be formed from CH_3Hg adsorbed to inorganic and organic reduced sulfur surfaces.

Result and Discussion

To test if $(\text{CH}_3)_2\text{Hg}$ could be formed from CH_3Hg on reduced sulfur surfaces, we initially adsorbed CH_3Hg to disordered Mackinawite ($\text{FeS}_m(s)$) in degassed purified water under low oxygen atmosphere and quantified the amount of $(\text{CH}_3)_2\text{Hg}$ formed. During the 1 h long experiment, we detected 0.37 ± 0.08 (0–20 min), 0.21 ± 0.07 (20–40 min) and 0.16 ± 0.07 (40–60 min) pmol of $(\text{CH}_3)_2\text{Hg}$ formed from 2.3 nmol of CH_3Hg (Supplementary Table S1). Control experiments with water and filtered $\text{FeS}_m(s)$ slurry ($0.02 \mu\text{m}$) did not produce detectable levels of $(\text{CH}_3)_2\text{Hg}$ supporting its formation from CH_3Hg adsorbed onto $\text{FeS}_m(s)$ particles.

In the present experiment, CH_3Hg was the only methyl containing compound and therefore acted as both the methyl donor and acceptor. The reaction could therefore involve either two CH_3Hg molecules adsorbed on neighboring sulfide groups or one molecule adsorbed reacting with a molecule in solution. To test this, we measured the formation of $(\text{CH}_3)_2\text{Hg}$ at $\text{CH}_3\text{Hg}:\text{FeS}_m(s)$ ratios ($\text{nmol} \cdot \mu\text{mol}^{-1}$) of 6.1, 1.8 and 0.38 by varying the concentration of CH_3Hg . $\text{FeS}_m(s)$ has been described as having a surface dominated by equal moles of mono and tri coordinated sulfide groups with the mono coordinated sulfide ($\equiv\text{Fe}_1\text{S}_1^-$) having stronger anionic properties¹⁹. We therefore assume these are the primary sites of CH_3Hg adsorption and calculated the fraction of $\equiv\text{Fe}_1\text{S}_1^-$ groups occupied by CH_3Hg in the experiment. We observed a greater fraction of CH_3Hg methylated at higher $\text{CH}_3\text{Hg}:\text{FeS}_m(s)$ ratios; i.e. where a higher percent of $\equiv\text{Fe}_1\text{S}_1^-$ sites are saturated (Fig. 1). The fraction of CH_3Hg in solution did not differ between the tests (Supplementary Fig. S1). This suggests the fraction methylated to be dependent on the number of sites occupied rather than concentration of CH_3Hg remaining in solution. Additional experiments covering a wider range of $\text{CH}_3\text{Hg}:\text{FeS}_m(s)$ ratios ($3.4 \cdot 10^{-2}$ to $3.4 \cdot 10^4 \text{ nmol} \cdot \mu\text{mol}^{-1}$), obtained by varying the concentration of $\text{FeS}_m(s)$, demonstrated that the fraction of CH_3Hg that was methylated increased as more $\equiv\text{Fe}_1\text{S}_1^-$ sites were occupied, and then decreased after the number of $\equiv\text{Fe}_1\text{S}_1^-$ groups were saturated with CH_3Hg , and the fraction of CH_3Hg bound decreased (Fig. 2). Both our experiments thus support a reaction mechanism involving two CH_3Hg molecules adsorbed on neighboring sulfide groups rather than a reaction involving one CH_3Hg molecule adsorbed on the surface and one molecule in solution.

$\text{FeS}_m(s)$ is the first mineral formed from environmental precipitation of $\text{S}^{2-}(aq)$ and $\text{Fe}^{2+}(aq)$; e.g. in sediment pore water and inside bacterial cells, and is the precursor to more stable FeS forms; e.g. greigite ($\text{Fe}_3\text{S}_4(s)$) and pyrite ($\text{FeS}_2(s)$)²⁰. Experiments with other, more stable, sulfide minerals ($\text{CdS}(s)$ and $\text{HgS}(s)$), showed similar fractions of CH_3Hg conversion to $(\text{CH}_3)_2\text{Hg}$ suggesting that the internal stability of the mineral is of minor importance (Supplementary Table S2). In a similar manner, the aging of $\text{FeS}_m(s)$ did not affect the fraction methylated (Supplementary Table S3).

Based on the above discussed results, we propose a $\text{S}_\text{N}2$ -type reaction for the formation of $(\text{CH}_3)_2\text{Hg}$ from CH_3Hg adsorbed onto sulfide mineral surfaces (Fig. 3). After adsorption of CH_3Hg onto the surface, the reaction is initiated by a nucleophilic attack of one of the CH_3Hg holding sulfur atoms on a Hg atom of a CH_3Hg molecule adsorbed on a neighboring sulfide site. The intermediate formed is then rearranged resulting in, as final products, one $(\text{CH}_3)_2\text{Hg}$ molecule and incorporation (co-precipitation) of the other Hg atom, becoming bound to two sulfur atoms at the surface of the sulfide mineral. For the reaction of CH_3Hg with $\text{FeS}_m(s)$, previous spectroscopic studies of Hg^{2+} adsorbed to $\text{FeS}_m(s)$ suggest that the Hg atom could either remain on the surface of the mineral or be precipitated as metacinnabar, $\beta\text{-HgS}(s)$ (and Fe^{2+} be released into the solution)^{21,22}. Which of these two end products would dominate in our experiment remains unclear as the final presumed $\text{Hg}^{2+}:\text{FeS}_m(s)$ is

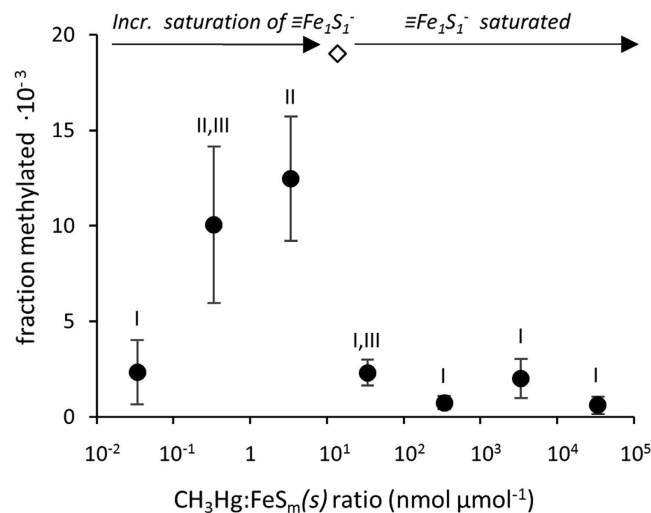


Figure 2. Methylation of CH_3Hg at different $\text{CH}_3\text{Hg}:\text{FeS}_m(s)$ ratios. Fraction of CH_3Hg methylated at $\text{CH}_3\text{Hg}:\text{FeS}_m(s)$ ratios ($\text{nmol } \mu\text{mol}^{-1}$) of $3.4 \cdot 10^{-2}$ to $3.4 \cdot 10^4$ and the theoretical saturation point of $\equiv\text{Fe}_1\text{S}_1^-$ groups on the $\text{FeS}_m(s)$ surface (diamond). Roman numerals indicate significant differences ($p < 0.05$).

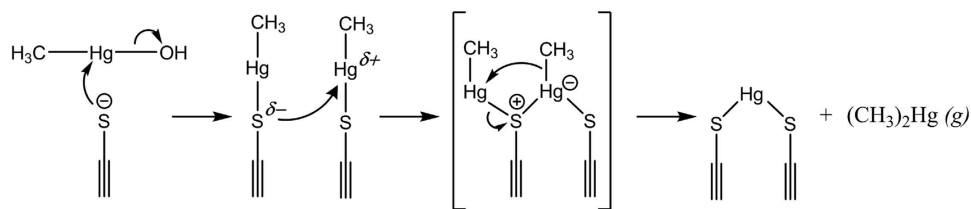


Figure 3. Proposed reaction mechanism. The proposed $\text{S}_\text{N}2$ -type reaction mechanism for the formation of $(\text{CH}_3)_2\text{Hg}$ from CH_3Hg mediated by inorganic or organic surfaces with neighboring reduced sulfur groups.

lower than in the previous studies, and furthermore, a significant fraction of added Hg is likely still remaining as CH_3Hg adsorbed onto the $\text{FeS}_m(s)$. Calculations of the equilibrium constant and the ΔG for the overall reaction of CH_3Hg and $\text{FeS}_m(s)$ with $(\text{CH}_3)_2\text{Hg}$ and $\text{HgS}(s)$ as end-products supports that the reaction is thermodynamically favorable (see supplementary discussion).

We also tested the previously demonstrated methylation pathway involving $\text{CH}_3\text{Hg}(aq)$ and dissolved sulfide¹⁵ and compared it to the reaction mediated by $\text{FeS}_m(s)$. The ratio $\text{CH}_3\text{Hg}:\text{S}^{2-}$ was varied from the optimum molar ratio of 2 ($2 \text{CH}_3\text{Hg}(aq) + \text{S}^{2-}(aq) \rightarrow \text{HgS}(s) + (\text{CH}_3)_2\text{Hg}(g)$) to that matching the $\text{CH}_3\text{Hg}:\text{FeS}_m(s)$ experiments ($4.3 \text{ nmol } \mu\text{mol}^{-1}$). The fraction CH_3Hg methylated with $\text{S}^{2-}(aq)$ was 6–40 times lower than the fraction methylated on $\text{FeS}_m(s)$ (Fig. 4). The geometry of the $(\text{CH}_3\text{Hg})_2\text{S}$ molecule should theoretically limit the transfer of the methyl group between Hg atoms bound to the same S (given the linearity of the S-Hg-C bond). We found the activation energy, E_a , for the formation of $(\text{CH}_3)_2\text{Hg}$ from the reaction of CH_3Hg with $\text{S}^{2-}(aq)$ and $\text{FeS}_m(s)$ to be 41 ± 6.8 and $91 \pm 4.6 \text{ kJ mol}^{-1}$, respectively (Supplementary Fig. S2). This suggests that the reaction with dissolved sulfide is slower due to a limited number of CH_3Hg molecules close enough for transfer of the methyl group to occur. The previously proposed reaction mechanism for the observed formation of $(\text{CH}_3)_2\text{Hg}$ in pure cultures of sulfate reducing bacteria, and in sediment amended with $\text{CH}_3\text{Hg}(aq)$ and purged with $\text{H}_2\text{S}(g)$, involves $(\text{CH}_3\text{Hg})_2\text{S}(s)$ as an intermediate^{14,15}. Given that surfaces with reduced sulfide would also be present in such experimental systems, we suggest that even though $(\text{CH}_3\text{Hg})_2\text{S}(s)$ has been observed when reacting $\text{CH}_3\text{Hg}(aq)$ with H_2S in water and when CH_3Hg was added to a subsample of the cell cultures, formation of $(\text{CH}_3)_2\text{Hg}$ by the mechanism proposed here is also a possible explanation for the $(\text{CH}_3)_2\text{Hg}$ produced in those previous experiments.

Experiments conducted from pH 6 at which most $\equiv\text{Fe}_1\text{S}_1^-$ groups would be protonated, to pH 8 where they would be deprotonated¹⁹, showed no difference in $(\text{CH}_3)_2\text{Hg}$ formation (Supplementary Fig. S3). Further, experiments conducted at ionic strengths of 0.017 and 0.20 M (NaCl) demonstrated that ionic strength did not impact the methylation. Adsorption studies of inorganic Hg onto $\text{FeS}_m(s)$ at different pH levels have shown no significant difference in the amount of inorganic Hg adsorbed even though small differences in the dissolved fraction were observed²³. Our results showing that $(\text{CH}_3)_2\text{Hg}$ formation rate is independent of pH and ionic strength are consistent with the high binding capacity of $\text{FeS}_m(s)$ for Hg compounds in both acidic and basic conditions and the fact that the reaction between CH_3Hg and $\text{FeS}_m(s)$ is a surface mediated process.

Reactive sites containing multiple thiol groups located on the surface of proteins are known to be important adsorption sites for heavy metals, including Hg²⁴. To test if $(\text{CH}_3)_2\text{Hg}$ could also be formed from CH_3Hg

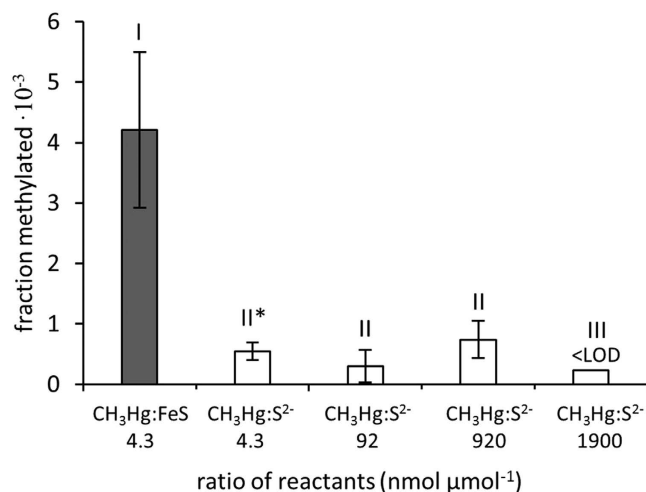


Figure 4. Methylation of CH₃Hg with S²⁻ (aq). Fraction of CH₃Hg methylated on FeS_m(s) (±SD, n = 3) at a CH₃Hg:FeS_m(s) ratio of 4.3 (nmol μmol⁻¹) or with dissolved sulfide at CH₃Hg:S²⁻ ratios of 4.3 to 1900 (nmol μmol⁻¹). LOD = Limit of detection. Roman numerals indicate significant differences (p < 0.05). *One outlier removed (n = 2).

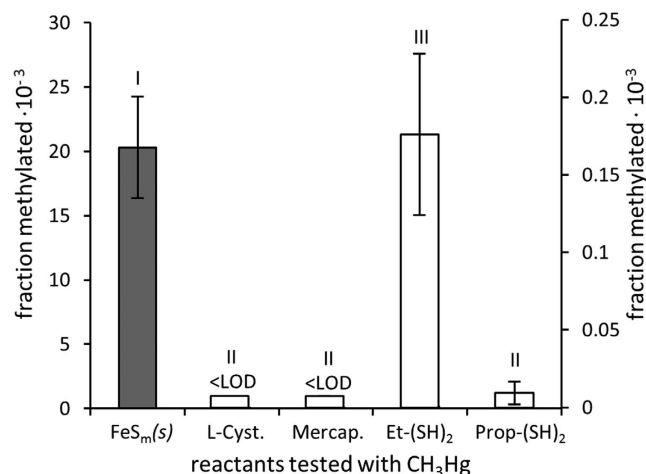


Figure 5. Methylation of CH₃Hg complexed with organic thiols. Fraction of CH₃Hg methylated (±SD, n = 3) on FeS_m(s) (CH₃Hg:FeS_m(s) ratio of 3.4 nmol μmol⁻¹, left hand axis) or with L-Cysteine (L-Cyst.), 3-mercaptopropionic acid (Mercap.), 1,2-ethanedithiol (Et-(SH)₂) or 1,3-propanedithiol (Prop-(SH)₂) (CH₃Hg:thiol ratio of 1000 and 2000 nmol μmol⁻¹ for mono- and dithiols respectively giving a CH₃Hg:R-SH ratio of 1 for both mono and di-thiols, right hand axis), right hand axis). LOD = Limit of detection. Roman numerals indicate significant differences (p < 0.05).

adsorbed onto neighboring thiol groups, we reacted CH₃Hg with two dithiol compounds (1,2-ethanedithiol and 1,3-propanedithiol) and two monothiol compounds (L-cysteine and 3-mercaptopropionic acid) at CH₃Hg:R-SH ratios of 1:1. We detected methylation of CH₃Hg using the dithiols but not with the monothiols (i.e. fraction methylated < 7.2 · 10⁻⁶) (Fig. 5). The higher methylation observed using 1,2-ethanedithiol compared to 1,3-propanedithiol could be due to a longer distance between the thiols of the latter. The fraction of CH₃Hg being methylated was two orders of magnitude lower when the reaction was mediated by 1,2-ethanedithiol compared to FeS_m(s). The sulfidic mineral surfaces will have a higher density of electrons in comparison to alkane dithiols, which should be favorable for the proposed reaction (Fig. 3). We used simple organic dithiols here as analogs for protein sites with multiple thiol groups as previous work have shown Hg²⁺ to complex proteins and natural organic matter via thiol groups as a bicoordinated complex (RS-Hg-SR)^{24,25}. The reactivity and symmetry (which is likely more flexible in proteins) are likely different between alkane dithiols and active sites on proteins. Nonetheless, our results show the potential for the formation of (CH₃)₂Hg from CH₃Hg adsorbed on neighboring protein thiol groups. We speculate that the higher methylation rate mediated by sulfide minerals suggests that this reaction could be more favorable on iron sulfur clusters (e.g. Fe₂S₂, Fe₃S₄, Fe₄S₄) present in certain proteins^{26,27} compared to protein thiols. We examined the potential for the reaction to occur in artificial sea water

in presence of diatom algae cells (*Thalassiosira weissflogii*) by comparing the formation of $(\text{CH}_3)_2\text{Hg}$ in pure sea water or in sea water with the presence of whole cells, cellular membrane material and organelles (i.e. nuclei and mitochondria settled at the g forces used here), or the remaining cytoplasm (Supplementary Fig. S4). In all cases, while $(\text{CH}_3)_2\text{Hg}$ was formed, the rate of formation was lower (8.6, 1.4 and 2.5 times in the presence of whole cells, cellular membrane material and organelles, respectively) than for $\text{FeS}_m(s)$ in seawater without organic matter present. The lower methylation in presence of plankton organic matter may be the result of an increase in the competition of CH_3Hg binding to sites less reactive for the methylation process. The results however demonstrate the potential for the above outlined mechanism to occur on FeS-clusters within cells after assimilation of CH_3Hg from marine waters.

Our study is the first to demonstrate the formation of $(\text{CH}_3)_2\text{Hg}$ from CH_3Hg adsorbed onto sulfide mineral surfaces or organic dithiols (CH_3Hg methylation rates up to $0.012 \pm 0.004 \times 10^{-3}$ detected, Fig. 1). In the ocean, the highest concentrations of $(\text{CH}_3)_2\text{Hg}$ are typically found in low oxygen environments where active degradation of organic matter is occurring, or in regions of concentrated biological material, as well as in the deep ocean^{1,2}. The relatively high degradation rate of $(\text{CH}_3)_2\text{Hg}$ observed in marine waters suggests it must be continually produced in the water column, sediments or in association with hydrothermal systems⁷. The formation of $(\text{CH}_3)_2\text{Hg}$ has mainly been hypothesized to be bacterially mediated, however direct experimental support for this assertion is missing²⁸. Further, the *in vivo* mechanism by which the $(\text{CH}_3)_2\text{Hg}$ could be produced inside the bacterial cells has not been identified¹⁴. We propose that the reaction pathway discussed above may be important abiotic as well as biotic pathways for formation of $(\text{CH}_3)_2\text{Hg}$ in the oceanic system. In addition to methylation of CH_3Hg in the presence of biological material via pathway involving the binding of CH_3Hg to thiols and the proposed methyl transfer reactions outlined above, there is also the potential for these reactions to occur in the presence of metal-sulfide particles within marine aggregates, or in the sulfide particles that are associated with hydrothermal vent plumes. The presence of reduced sulfur in the upper ocean has been shown in numerous studies^{29,30}. There is also evidence for reducing conditions within sinking marine aggregates, and the presence of $\text{CdS}(s)$ in low oxygen sub-thermocline ocean waters^{31,32}. Finally, there is substantial evidence for metal sulfide and pyrite particulates emanating from hydrothermal vents³³. Although the concentrations of CH_3Hg in our experiments exceed the concentrations found in marine waters, our ratio of CH_3Hg to sulfide mineral surface area are similar to the ratio expected on particles or inside planktonic cells present in the ocean. For example, for the low oxygen waters in the North Atlantic, where observed concentration of particulate Cd has been assumed to mainly be composed of $\text{CdS}(s)$, calculated particulate $\text{CH}_3\text{Hg}:\text{Cd}$ is about 10^{-3} (molar basis)^{34,35}. Furthermore, inside planktonic cells the molar $\text{CH}_3\text{Hg}:\text{Fe}$ ratio of 10^{-3} to 10^{-4} is typically found but the expected $\text{CH}_3\text{Hg}:\text{FeS}$ is lower given that not all intracellular Fe would occur as FeS-clusters^{8,36,37}. Reported rates of $(\text{CH}_3)_2\text{Hg}$ formation in marine water are scant. Lehnerr *et al.* reported potential CH_3Hg methylation rates, producing $(\text{CH}_3)_2\text{Hg}$, of up to $1.6 \cdot 10^{-3} \text{ d}^{-1}$ for Arctic waters²⁸. The fraction of CH_3Hg converted to $(\text{CH}_3)_2\text{Hg}$ in our experiments (up to $20 \cdot 10^{-3}$ in purified water and up to $15 \cdot 10^{-3}$ in artificial sea water, Fig. 5 and Supplementary Fig. S4) for experiments carried out within 24 h are an order of magnitude higher than the methylation rates observed by Lehnerr *et al.* We propose that the reactions outlined above could produce a significant portion of the $(\text{CH}_3)_2\text{Hg}$ within the upper ocean water column, primarily in association with organic matter recycling. In the deep ocean, the elevated concentrations of total Hg, CH_3Hg , as well as dissolved and colloidal Fe, found during the Geotraces GA03 cruise in the vicinity of the mid-Atlantic Ridge^{34,38}, compared to other deep ocean waters, suggest that hydrothermal vent plumes are environments where $(\text{CH}_3)_2\text{Hg}$ could be formed by reactions mediated by FeS surfaces.

Material and Methods

The preparation of sulfide minerals and all experiments were conducted under a $\text{N}_2(g)$ or $\text{Ar}(g)$ atmosphere and using degassed ($\text{N}_2(g)$ or $\text{Ar}(g)$ purged) purified water ($\Omega < 18.2$). Disordered Mackinawite ($\text{FeS}_m(s)$) was prepared by adding 100 ml of 0.6 M Na_2S to 100 ml of 0.6 M Morh's salt ($(\text{NH}_4)_2\text{Fe}(\text{II})(\text{SO}_4)_2 \cdot 6\text{H}_2\text{O}$)³⁹. The precipitated crystals of $\text{FeS}_m(s)$ were aged for 0 h, 1 day and 7 days, then collected by centrifugation (5 min, 2.6 kG) and washed three times with purified water. Since the aging of $\text{FeS}_m(s)$ has previously been shown to significantly stop at -80°C ³⁹, the final product was re-suspended in water, subsampled into smaller vials and stored in a N_2 atmosphere at -80°C until use. For experiments where the activity of $\text{FeS}_m(s)$ was compared to that of $\text{CdS}(s)$ and $\text{HgS}(s)$ (Supplementary Table S2), $\text{FeS}_m(s)$ was prepared as described above (25 ml of 0.6 M Na_2S and 0.6 M of Morh's salt), and at the same time, $\text{CdS}(s)$ and $\text{HgS}(s)$ were synthesized by adding 25 ml or 15 ml of 0.6 M Na_2S to 25 ml of 0.6 M $\text{Cd}(\text{NO}_3)_2 \cdot 4\text{H}_2\text{O}$ or 15 ml 0.6 M HgCl_2 (prepared by dissolving $\text{HgCl}_2(s)$ using 700 μL HCl following dilution in purified water), respectively. For $\text{CdS}(s)$ precipitated with excess of Cd, this was prepared by adding 12.5 ml of 0.6 M Na_2S and 12.5 ml degassed MQ water to 25 ml 0.6 M $\text{Cd}(\text{NO}_3)_2 \cdot 4\text{H}_2\text{O}$. The precipitated crystals were collected by centrifugation (5 min, 2.6 kG), and washed four times until excess acid in the $\text{HgS}(s)$ slurry was removed (pH ~ 7). A subsample of each was freeze-dried to calculate the concentration (weight to weight) of stock slurries, and characterized using X-ray Diffraction Crystallography (XRD) and Brunauer–Emmett–Teller (BET) (Supplementary Table S4, Fig. S5 and discussion).

Formation of $(\text{CH}_3)_2\text{Hg}$ was tested by adding $\text{CH}_3\text{Hg}(aq)$ to $\text{FeS}_m(s)$, $\text{CdS}(s)$, $\text{HgS}(s)$, $\text{S}^{2-}(aq)$, L-Cysteine, 3-mercaptopropionic acid, 1,2-ethanedithiol or 1,3-propanedithiol in acid cleaned glass vials (total volume of 42 cm^3). The amount of thiol ligand, CH_3Hg and final volume of solution used is summarized in Supplementary Table S5. Each experimental set was done in triplicate and the $\text{CH}_3\text{Hg}(aq)$ standard was prepared from a 1000 ppm $\text{CH}_3\text{Hg}(aq)$ stock solution (pH 1, Alfa Aesar) and pH was adjusted to ~ 6 – 8 using 2–8 M $\text{KOH}(aq)$. The produced $(\text{CH}_3)_2\text{Hg}(g)$ was collected onto CarbotrapTM (Supelco) solid absorbent either by purging the headspace of the vial with 200 ml/min of Argon (Ar) while gently stirring the solution with a magnetic stirring bar (results presented as formation rates, i.e. $n(\text{CH}_3)_2\text{Hg}(g)$ (pmol) $\cdot n\text{CH}_3\text{Hg}$ added (pmol)⁻¹ $\cdot \text{time}$ (min)⁻¹), or by sampling 0.1–5 ml of the headspace from a closed vial through the septa using a syringe. For the latter, the total concentration of $(\text{CH}_3)_2\text{Hg}$ was calculated based on the relative volumes of water and gas, the sampled volume of gas and the dimensionless

Henry solubility constant (H^c ; concentration in the aqueous phase \cdot concentration in the gas phase $^{-1}$) for $(CH_3)_2Hg^{40}$, and results are presented as fraction of CH_3Hg methylated (i.e. $n(CH_3)_2Hg(g)$ (pmol) \cdot nCH_3Hg added (pmol) $^{-1}$). In the initial experiment, the $FeS_m(s)$ slurry was filtered through a 0.02 μm PTFE syringe filter and the control experiment done by adding 2.3 nmol of CH_3Hg to 1 ml of the filtrate. The percent of $\equiv Fe_1S_1^-$ with CH_3Hg adsorbed was calculated from the concentration of $CH_3Hg(aq)$ immobilized in a separate adsorption experiment (Supplementary Fig. S1), the specific surface area of $FeS_m(s)$ (Supplementary Table 3) and assuming two $\equiv Fe_1S_1^-$ groups nm^{-2} ¹⁹. The activation energy, E_a (kJ/mol), for the formation of $(CH_3)_2Hg$ was determined assuming a pseudo first order reaction and using the Arrhenius Equation ($\ln k = \ln Ae - E_a/RT$; rate constant (k), frequency factor (Ae), activation energy (E_a), gas constant (R), temperature (T ; in kelvin) from experiments conducted at 0, 18, 40 and 60 °C ($n = 3$, details are provided in Supplementary Table S5). The activation energy (including standard deviation) was calculated from the slope of $\ln k$ vs. $1/T$ (slope = $-E_a/R$). For CH_3Hg on $FeS_m(s)$, no $(CH_3)_2Hg(g)$ was detected in samples incubated at 0 °C hence the production of $(CH_3)_2Hg$ during the cooling process was neglected. For the reaction with S^{2-} (where a higher concentration of CH_3Hg was used), the $(CH_3)_2Hg$ formed was similar at 0 and 18 °C. The E_a was thus calculated only using the results obtained at 40 and 60 °C.

When the reaction vessels were purged, sampled gas was first dried on a soda lime trap placed in line with the CarbotrapTM column, and when the headspace was sampled, the gas was injected directly on the CarbotrapTM column via an injection valve. Collected $(CH_3)_2Hg(g)$ was then thermally desorbed and separated by isothermal gas chromatography before being pyrolytically decomposed to Hg^0 and detected using CVAFS (Tekran, model 2500). External calibration was done using known amounts of synthesized $(CH_3)_2^{200}Hg(aq)$ standard purged onto CarbotrapTM columns. The $(CH_3)_2^{200}Hg$ was manufactured in house from $^{200}HgCl_2$ and 3 M methyl magnesium chloride in tetrahydrofuran (Supplementary Method). WARNING, Extreme caution is needed when synthesizing $(CH_3)_2Hg$ as it is a volatile and extremely toxic compound! Even small amounts absorbed through the skin have proven fatal! Due to variations in the concentration of $(CH_3)_2Hg$ in the diluted aqueous standard prepared from synthesized stock solution, standards were prepared daily and the concentration was determined by collecting purgeable Hg from the standard on to a gold trap and using a second calibration of 10–200 μl of $Hg^0(g)$ at a known temperature (also purged onto gold traps). Detection limits were calculated from the amount of $(CH_3)_2Hg$ detected from experimental replicates utilizing equimolar concentrations of $CH_3Hg(aq)$ ($n = 3$, mean + 2SD).

Adsorption of $CH_3Hg(aq)$ onto $FeS_m(s)$ was tested by incubating 0.70 ($n = 1$), 2.8 ($n = 1$) and 11 ($n = 1$) nmol of CH_3Hg with 2.8 μmol $FeS_m(s)$ in 0.6 ml of DI in a disposable syringe. The samples were left for up to 60 minutes and the dissolved fraction was then collected using a 0.02 μm syringe filter. In a second experiment, 0.34 nmol CH_3Hg was added to 50 μmol of $FeS_m(s)$ in 10 ml degassed DI. The samples were filtered after an equilibration time of 10 min, 60 min or 24 h using 0.05 μm membrane filters. The amount of CH_3Hg remaining in solution was quantified using EPA method 1630 with an automated analyzer (Tekran 2700). Statistical analysis was conducted using IBM SPSS statistics. All data (fraction methylated or methylation rates) were log transformed before analysis of variance followed by Tukey's post-hoc test. For non-normally distributed log transformed data, median test following a pairwise t-test approach was performed.

References

- Fitzgerald, W. F., Lamborg, C. H. & Hammerschmidt, C. R. Marine Biogeochemical Cycling of Mercury. *Chem. Rev.* **107**, 641–662 (2007).
- Mason, R. P. & Fitzgerald, W. F. Alkylmercury species in the equatorial Pacific. *Nature* **347**, 457–459 (1990).
- Cossa, D., Coquery, M., Gobeil, C. & Martin, J.-M. In *Reg. Glob. cycles Mercur. Sources, fluxes, mass Balanc.* (Baeyens, R., Edinghaus, R. & Vasiliev, O.) 229–247 (1996).
- Conaway, C. H. *et al.* Dimethylmercury in coastal upwelling waters, Monterey Bay, California. *Environ. Sci. Technol.* **43**, 1305–1309 (2009).
- Mason, R. P. *et al.* Mercury biogeochemical cycling in the ocean and policy implications. *Environ. Res.* **119**, 101–117 (2012).
- Kirk, J. L. *et al.* Mercury in Arctic marine ecosystems: sources, pathways and exposure. *Environ. Res.* **119**, 64–87 (2012).
- Morel, F. M. M., Kraepiel, A. M. L. & Amyot, M. The Chemical Cycle and Bioaccumulation of Mercury. *Annu. Rev. Ecol. Syst.* **29**, 543–566 (1998).
- Mason, R. P., Reinfelder, J. R. & Morel, F. M. M. Uptake, toxicity, and trophic transfer of mercury in a coastal diatom. *Environ. Sci. Technol.* **30**, 1835–1845 (1996).
- Mason, R. P. & Fitzgerald, W. F. The distribution and biogeochemical cycling of mercury in the equatorial Pacific Ocean. *Deep Sea Res. Part I* **40**, 1897–1924 (1993).
- Baya, P. A., Gosselin, M., Lehnher, I., Louis, V. L. S. & Hintelmann, H. Determination of monomethylmercury and dimethylmercury in the arctic marine boundary layer. *Environ. Sci. Technol.* **49**, 223–232 (2015).
- Jensen, S. & Jernelov, A. Biological methylation of mercury in aquatic organisms. *Nature* **223**, 753–754 (1969).
- Parks, J. M. *et al.* The genetic basis for bacterial mercury methylation. *Science* **339**, 1332–1335 (2013).
- Benoit, J. M., Gilmour, C. C. & Mason, R. P. Aspects of bioavailability of mercury for methylation in pure cultures of *desulfobulbus propionicus* (1pr3). *Appl. Environ. Microbiol.* **67**, 51–58 (2001).
- Baldi, F., Pepi, M. & Filippelli, M. Methylmercury Resistance in *Desulfobulbus propionicus* Strains in Relation to Methylmercury Degradation. *Appl. Environ. Microbiol.* **59**, 2479–2485 (1993).
- Craig, P. J. & Bartlett, P. D. The role of hydrogen sulfide in environmental transport of mercury. *Nature* **275**, 635–637 (1978).
- Khan, M. A. & Wang, F. Chemical demethylation of methylmercury by selenoamino acids. *Chem. Res. Toxicol.* **23**, 1202–1206 (2010).
- Imura, N., Sukegawa, E., Pan, S.-K., Nagao, K. & Kim, J.-Y. Methylation of inorganic mercury with methylcobalamin, a vitamin B12 analog. *Science* **172**, 1248–1249 (1971).
- Asaduzzaman, A. M. & Schreckenbach, G. Degradation mechanism of methyl mercury selenoamino acid complexes: a computational study. *Inorg. Chem.* **50**, 2366–2372 (2011).
- Wolthers, M., Charlet, L., van Der Linde, P. R., Rickard, D. & van Der Weijden, C. H. Surface chemistry of disordered mackinawite (FeS). *Geochim. Cosmochim. Acta* **69**, 3469–3481 (2005).
- Rickard, D. & Luther, G. W. *Chemistry of iron sulfides*. *Chem. Rev.* **107** (2007).
- Skyllberg, U. & Drott, A. Competition between disordered iron sulfide and natural organic matter associated thiols for mercury(II)-an EXAFS study. *Environ. Sci. Technol.* **44**, 1254–1259 (2010).

22. Jeong, H. Y., Klaue, B., Blum, J. D. & Hayes, K. F. Sorption of mercuric ion by synthetic nanocrystalline mackinawite (FeS). *Environ. Sci. Technol.* **41**, 7699–7705 (2007).
23. Liu, J., Valsaraj, K. T., Devai, I. & DeLaune, R. D. Immobilization of aqueous Hg(II) by mackinawite (FeS). *J. Hazard. Mater.* **157**, 432–440 (2008).
24. DeSilva, T. M., Veglia, G., Porcelli, F., Prantner, A. M. & Opella, S. J. Selectivity in heavy metal-binding to peptides and proteins. *Biopolymers* **64**, 189–197 (2002).
25. Skyllberg, U., Bloom, P. R., Qian, J., Lin, C. M. & Bleam, W. F. Complexation of mercury(II) in soil organic matter: EXAFS evidence for linear two-coordination with reduced sulfur groups. *Environ. Sci. Technol.* **40**, 4174–4180 (2006).
26. Beinert, H., Holm, R. H. & Munch, E. Iron-sulfur clusters: nature's modular, multipurpose structures. *Science*. **277**, 653–659 (1997).
27. Rouault, T. A. & Tong, W.-H. Iron-sulphur cluster biogenesis and mitochondrial iron homeostasis. *Nat. Rev. Mol. Cell Biol.* **6**, 345–351 (2005).
28. Lehnher, I., St. Louis, V. L., Hintelmann, H. & Kirk, J. L. Methylation of inorganic mercury in polar marine waters. *Nat. Geosci.* **4**, 298–302 (2011).
29. Cutter, G. A. & Krahnforst, C. F. Sulfide in surface waters of the western Atlantic ocean. *Geophys. Res. Lett.* **15**, 1393–1396 (1988).
30. Luther, G. W. & Tsamakis, E. Concentration and form of dissolved sulfide in the oxic water column of the ocean. *Mar. Chem.* **27**, 165–177 (1989).
31. Janssen, D. J. *et al.* Undocumented water column sink for cadmium in open ocean oxygen-deficient zones. *Proc. Natl. Acad. Sci.* **111**, 6888–6893 (2014).
32. Balzano, S., Statham, P. J., Pancost, R. D. & Lloyd, J. R. Role of microbial populations in the release of reduced iron to the water column from marine aggregates. *Aquat. Microb. Ecol.* **54**, 291–303 (2009).
33. Yücel, M., Gartman, A., Chan, C. S. & Luther, G. W. Hydrothermal vents as a kinetically stable source of iron-sulphide-bearing nanoparticles to the ocean. *Nat. Geosci.* **4**, 367–371 (2011).
34. Bowman, K. L., Hammerschmidt, C. R., Lamborg, C. H. & Swarr, G. Mercury in the North Atlantic Ocean: The U.S. GEOTRACES zonal and meridional sections. *Deep. Res. Part II Top. Stud. Oceanogr.* **116**, 251–261 (2015).
35. Conway, T. M. & John, S. G. The cycling of iron, zinc and cadmium in the North East Pacific Ocean – Insights from stable isotopes. *Geochim. Cosmochim. Acta* **164**, 262–283 (2015).
36. Luengen, A. C. & Flegal, A. R. Role of phytoplankton in mercury cycling in the San Francisco Bay estuary. *Limnol. Oceanogr.* **54**, 23–40 (2009).
37. Eisler, R. *Compendium of Trace Metals and Marine Biota*. (Elsevier, 2009).
38. Fitzsimmons, J. N. *et al.* Partitioning of dissolved iron and iron isotopes into soluble and colloidal phases along the GA03 GEOTRACES North Atlantic Transect. *Deep. Res. Part II* **116**, 130–151 (2015).
39. Wolthers, M., Van Der Gaast, S. J. & Rickard, D. The structure of disordered mackinawite. *Am. Mineral.* **88**, 2007–2015 (2003).
40. Talmi, Y. & Mesmer, R. E. Studies on vaporization and halogen decomposition of methylmercury compounds using gc with a microwave detector. *Water Res.* 547–552 (1975).

Acknowledgements

This research was supported by the Swedish Research Council (International Postdoc grant 637-2014-54) to S.J. and partial support for N.M.M. and R.P.M. from the National Institutes of Health, through collaboration with investigators at Dartmouth College (NIH Grant Number P42 ES007373). We thank John Macharia and Andrew Meguerdichian in Dr. Steven Suib's group at the University of Connecticut for BET and XRD analysis. Axenic plankton culture was provided by the National Oceanic and Atmospheric Administration, Milford, US.

Author Contributions

S.J. and N.M.M. designed and carried out the experimental work; R.P.M. supervised the research; S.J., N.M.M. and R.P.M. wrote the paper.

Additional Information

Supplementary information accompanies this paper at <http://www.nature.com/srep>

Competing financial interests: The authors declare no competing financial interests.

How to cite this article: Jonsson, S. *et al.* Dimethylmercury Formation Mediated by Inorganic and Organic Reduced Sulfur Surfaces. *Sci. Rep.* **6**, 27958; doi: 10.1038/srep27958 (2016).



This work is licensed under a Creative Commons Attribution 4.0 International License. The images or other third party material in this article are included in the article's Creative Commons license, unless indicated otherwise in the credit line; if the material is not included under the Creative Commons license, users will need to obtain permission from the license holder to reproduce the material. To view a copy of this license, visit <http://creativecommons.org/licenses/by/4.0/>